Biophysics Reviews

RESEARCH ARTICLE | MAY 14 2026

A novel optoelectronic platform combining LED-driven pacing and laser optoporation for high-throughput cardiac electrophysiology

Chiara Florindi ; Carolina Scandellari ; Claudia Maniezzi ; Giulia Bruno ; Luca Sala ; Annarita Di Mise ; Guglielmo Lanzani ; Chiara Bertarelli ; Marcella Rocchetti ; Antonio Zaza ; Michele Dipalo ; Francesco Lodola

Biophysics Rev. 7, 021406 (2026)
https://doi.org/10.1063/5.0311976

A novel optoelectronic platform combining LED-driven pacing and laser optoporation for high-throughput cardiac electrophysiology

Cite as: Biophysics Rev. **7**, 021406 (2026); doi: 10.1063/5.0311976
Submitted: 13 November 2025 · Accepted: 14 April 2026 ·
Published Online: 14 May 2026

View Online Export Citation CrossMark

Chiara Florindi,[1,2,a)] Carolina Scandellari,[3] Claudia Maniezzi,[1] Giulia Bruno,[3] Luca Sala,[1,4] Annarita Di Mise,[1,4] Guglielmo Lanzani,[2,5] Chiara Bertarelli,[2,6] Marcella Rocchetti,[1] Antonio Zaza,[1] Michele Dipalo,[3] and Francesco Lodola[1,2,a)]

AFFILIATIONS

[1]Department of Biotechnology and Biosciences, University of Milano-Bicocca, Milan, Italy
[2]Center for Nano Science and Technology, Istituto Italiano di Tecnologia, Milan, Italy
[3]FORESEE Biosystems Srl, Genova, Italy
[4]Center for Cardiac Arrhythmias of Genetic Origin, Istituto Auxologico Italiano IRCCS, Milan, Italy
[5]Department of Physics, Politecnico di Milano, Milan, Italy
[6]Department of Chemistry, Materials and Chemical Engineering "Giulio Natta," Politecnico di Milano, Milan, Italy

[a)]**Authors to whom correspondence should be addressed:** c.florindi@campus.unimib.it and francesco.lodola@unimib.it

ABSTRACT

Reproducing the rhythmic electrical activity of the heart *in vitro* enables researchers to study how cardiomyocytes (CMs) respond to changes in pacing frequency in terms of contraction dynamics, electrical activity, and overall function. While electrical stimulation remains the gold standard, optical stimulation is emerging as a less invasive alternative with superior spatial and temporal resolution. Here, we propose a non-genetic, high-throughput optical platform for the stimulation of CMs cultured on microelectrode arrays, based on Ziapin2, a molecular phototransducer. Importantly, the system also incorporates a laser-based membrane poration module, allowing reliable access to intracellular signals. A user-friendly software was also developed for simultaneous analysis of multiple electrophysiological traces and to streamline data interpretation. Altogether, we propose a fully integrated, minimally invasive powerful platform for *in vitro* cardiac electrophysiology studies, with promising applications in disease modeling, drug screening, and fundamental research.

I. INTRODUCTION

The precise coordination of electrical activity in cardiomyocytes (CMs) is pivotal to rhythmic excitation–contraction coupling, thus to effective cardiac function.[1] Recapitulating these dynamics *in vitro* is essential for elucidating the electrophysiological properties of cardiac cells and for modeling both physiological and pathological states.[2–4] In this context, the use of well-defined pacing protocols markedly reduces the intrinsic variability associated with spontaneous contractions, but, more importantly, it enables systematic exploration of frequency-dependent electrophysiological phenomena.

Electrical stimulation has long served as the gold standard for pacing CMs *in vitro*, due to its precise temporal resolution and straightforward protocol standardization.[5] However, direct electrode contact is not without significant challenges: electrochemical artifacts at the electrode–electrolyte interface, progressive loss of stimulation fidelity due to electrode degradation or cellular debris accumulation, and inherent constraints in spatial resolution might occur, introducing substantial variability, particularly in chronic or high-throughput applications, thus complicating data interpretation and limiting practical scalability. Although contactless field stimulation mitigates some of these drawbacks, it often results in non-uniform electric field distribution and reduced spatial precision. Such limitations have driven growing interest in alternative, non-contact methods. Among these, optical stimulation has come to the forefront due to several key enabling features.[6–8]

Optical pacing offers clear advantages: it avoids the electrochemical and mechanical interference associated with electrodes, minimizing perturbation of the cells and allowing for unprecedented spatial

and temporal resolution. Yet, conventional optical pacing typically relies on optogenetic tools to render cardiac cells photosensitive, requiring genetic modifications that are not always feasible or desirable, especially in translational research and drug screening contexts, where genetic manipulation may alter cellular physiology or raise biosafety concerns.[8] Here, we introduce a fully integrated, optoelectronic platform for *in vitro* cardiac electrophysiology. This system combines non-genetic contactless and spatially precise optical pacing with laser-based poration to achieve intracellular access in human-induced pluripotent stem cells-derived CMs (hiPSC-CMs) cultured on microelectrode arrays (MEAs).[9–12] Pacing is achieved using an LED light source tuned to the peak absorption of Ziapin2, a small-molecule phototransducer that inserts into the plasma membrane. Upon illumination, Ziapin2 undergoes conformational changes that rapidly modulate membrane capacitance, inducing membrane potential perturbations.[13–15] Depending on the stimulation parameters and on the electrophysiological properties of the preparation, this photoresponse can remain subthreshold[16] or reach the threshold required for reliable action potential (AP) initiation.[17–20] In this framework, LED illumination provides simple, reproducible, and contactless stimulation.

Meanwhile, the laser poration protocol employs highly localized, minimally invasive laser pulses to transiently increase membrane permeability, enabling high-quality intracellular recordings without compromising cell viability or electrophysiological integrity. Combined, these technologies enable precise pacing and intracellular access, offering a comprehensive assessment of cellular electrophysiology. To fully exploit the capabilities of this multifunctional system, we developed a software for automated, simultaneous analysis of multiple electrophysiological traces, facilitating rapid interpretation of complex datasets and supporting scalable workflows. Altogether, the integration of non-genetic optical stimulation, laser poration, and automated data analysis represents a significant advance in the development of high-throughput *in vitro* cardiac platforms. The versatility and modularity of this approach render it particularly suited for applications in disease modeling, drug screening, and fundamental investigations in cardiac biophysics.

II. RESULTS AND DISCUSSION

A. Development of the optoelectronic platform

The IntraCell system (Foresee Biosystems) was originally developed to enable high-fidelity intracellular recordings from electrically excitable cells via laser poration, using cultures grown on planar MEAs.[11] To expand its capabilities toward active modulation of cardiac electrophysiology, we modified the platform by integrating an optical stimulation module. Specifically, we incorporated a 470 nm LED into the optical path of the system, creating a dual-modality setup capable of both intracellular signal acquisition and light-driven pacing from the same cellular preparation [Fig. 1(a)]. The LED wavelength was selected to match the excitation peak of Ziapin2, enabling effective

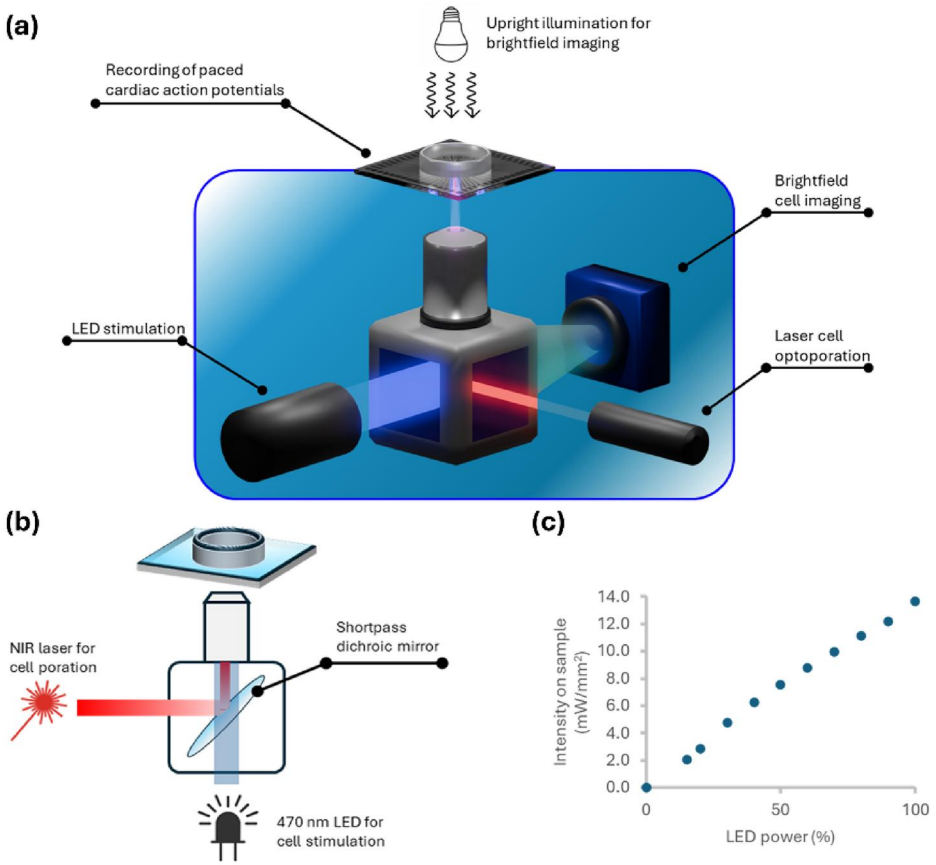

FIG. 1. Design and development of the optoelectronic platform. (a) Schematic representation of the optical setup integrating the laser optoporation and LED stimulation modules. The laser enables intracellular access for recording action potential-like signals, while the LED provides optical pacing. Brightfield illumination allows imaging of cells plated on the MEA. (b) Optical path schematic showing the integration of a dichroic mirror that co-aligns the blue LED with the laser axis, preventing interference with the near-infrared light used for optoporation. (c) Calibration curve of the LED power intensity delivered to the sample as a function of adjustable input settings.

light-induced modulation of cell membrane properties for non-genetic optical pacing in hiPSC-CMs. The optical path was engineered to deliver uniform illumination across the field of view of the brightfield camera used to image the cells, corresponding to approximately 700 μm in diameter, with precise alignment to avoid interference with the near-infrared (1064 nm) laser beam used for optoporation. A short-pass dichroic mirror (cutoff > 550 nm) was employed to co-align the blue LED beam with the laser axis while preserving independent control of the two light sources [Fig. 1(b)]. The LED output was collimated and focused to achieve homogeneous irradiance on the sample, with adjustable intensity up to ~14 mW/mm^2 [Fig. 1(c)]. Key stimulation parameters, including pulse duration, repetition rate, and timing, were controlled via Transistor-Transistor Logic (TTL) triggering, allowing precise synchronization with electrophysiological recordings. The stimulation system enables single or repeated light pulses with duration of single pulses from 100 μs to 5 s and repetition rate up to 5 kHz.

B. Electrophysiological recordings from hiPSC-CM cultures

To evaluate the efficacy of the optoelectronic platform, we tested its ability to induce electrical responses in hiPSC-CMs cultured on commercial 60-electrode MEAs and treated with 25 μM Ziapin2, a concentration previously validated in cardiac tissue [see protocol in Fig. 2(a)].[19] Baseline extracellular field potential recordings revealed spontaneous activity with an average beating rate (BR) of approximately 0.3 Hz. Upon pulsed blue-light illumination at 470 nm, corresponding to the excitation peak of Ziapin2, at an intensity of 14 mW/mm^2 and a stimulation frequency of 0.5 Hz, the cardiomyocytes reliably followed the imposed pacing [Fig. S1(a)]. This confirmed the capability of Ziapin2 to mediate non-genetic optical control of cardiac excitability *in vitro*. In contrast, vehicle-treated (dimethyl sulfoxide, DMSO) cultures showed no entrainment under identical stimulation conditions, excluding nonspecific photothermal or photomechanical effects of light exposure [Fig. S1(b)].

Following the extracellular recordings, we then assessed the platform's ability to access intracellular signals in the same Ziapin2-treated cultures using the IntraCell system's laser poration module controlled by the FB Alps suite (Fig. S2). The 1064 nm laser is precisely targeted to individual electrodes to induce localized membrane poration at the cell–electrode interface without disrupting adjacent sites. By tuning laser parameters (e.g., 40% power), we reliably converted extracellular field potential waveforms into intracellular-like APs, evidenced by a steep upstroke, sustained plateau phase, and

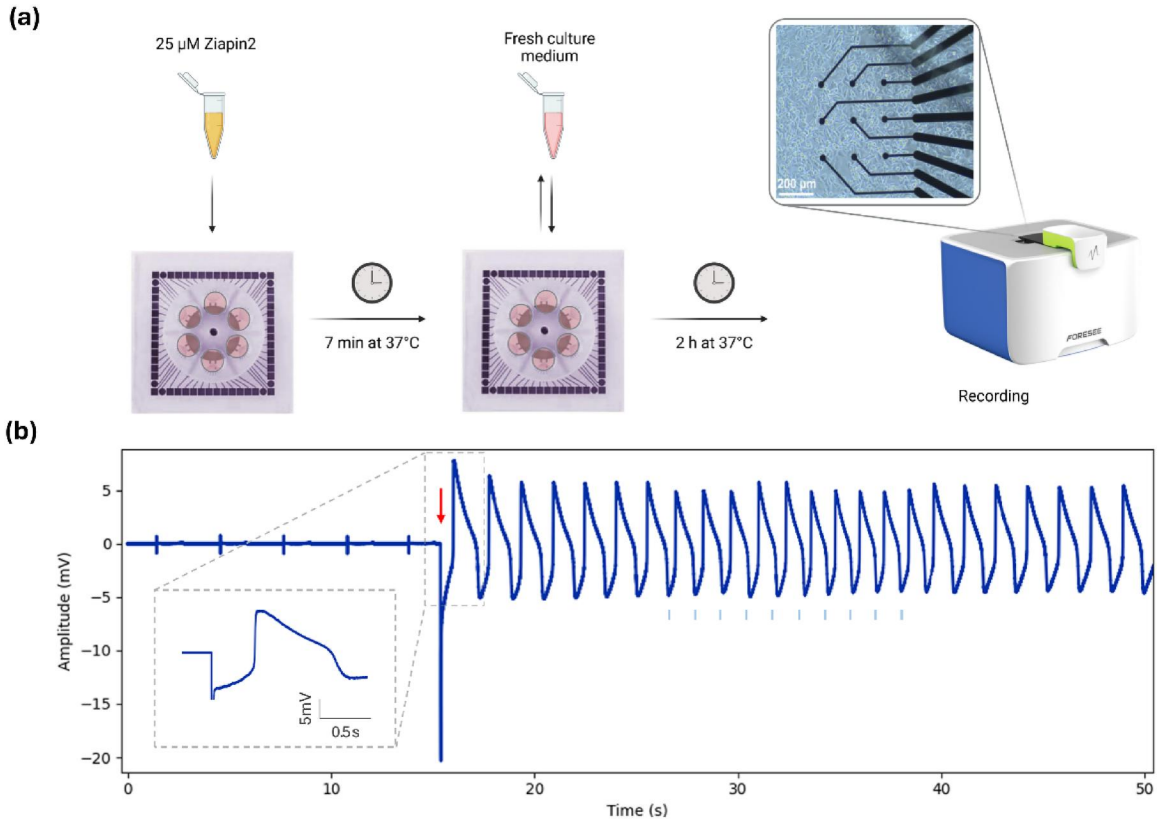

FIG. 2. Ziapin2 incubation and photostimulation of hiPSC-CMs. (a) Schematic representation of the Ziapin2 incubation (25 μM) and washout steps performed prior to MEA recordings, created in BioRender (https://BioRender.com/qhnv090). (b) Representative trace showing field potential recordings from hiPSC-CMs cultured on MEAs, along with intracellular signals obtained after laser poration (red arrow) and subsequent light stimulation (cyan dots; 1 Hz, 100 ms pulse duration, 100% LED power). Inset in (b): zoomed-in view of the exact moment of laser poration, highlighting the immediate artifact and transition dynamics. Recordings carried out at 37 °C.

repolarization phase [Fig. 2(b)]. This approach resulted in a substantial increase in signal amplitude, up to a fourfold relative to preporation extracellular recordings, producing AP waveforms that closely resemble those obtained from canonical intracellular recordings. Although the signal amplitude increases significantly after laser optoporation, the amplitude values should not be interpreted as absolute membrane potentials, since the cell–electrode coupling on MEA does not provide a high-resistance seal as in patch-clamp recordings.

The use of laser-induced APs enabled the extraction of electrophysiological characteristics not measurable with conventional extracellular MEA recordings. Specifically, we detected AP duration (APD) at different repolarization levels (APD_{30}, APD_{50}, and APD_{90}) and upstroke velocity (UV). This methodology thus provides a more accurate and comprehensive evaluation of cardiomyocyte electrophysiology. As can be observed in Fig. 2(b), after laser optoporation, the repolarization phase of the AP pulls the electrode potential level toward more negative potentials, as expected for intracellular-like signals. However, due to the hardware DC filtering intrinsic to all MEA acquisition systems, the electrode potential is slowly pulled back toward the baseline during the diastolic phase. This feature makes it challenging to infer information on the true resting membrane potential or the subthreshold ionic currents preceding AP firing, such as the funny current (I_f).

We then compared optical stimulation (LS) with Ziapin2 to conventional electrical pacing (ES), the gold standard for CM activation, using direct electrode stimulation on the same MEA platform. Both modalities were tested at stimulation frequencies of 0.5 Hz to evaluate the capability of Ziapin2-driven photoexcitation to sustain periodic activation (Fig. 3). Intracellular recordings revealed that optical stimulation reliably elicited APs comparable in morphology to those electrically evoked.

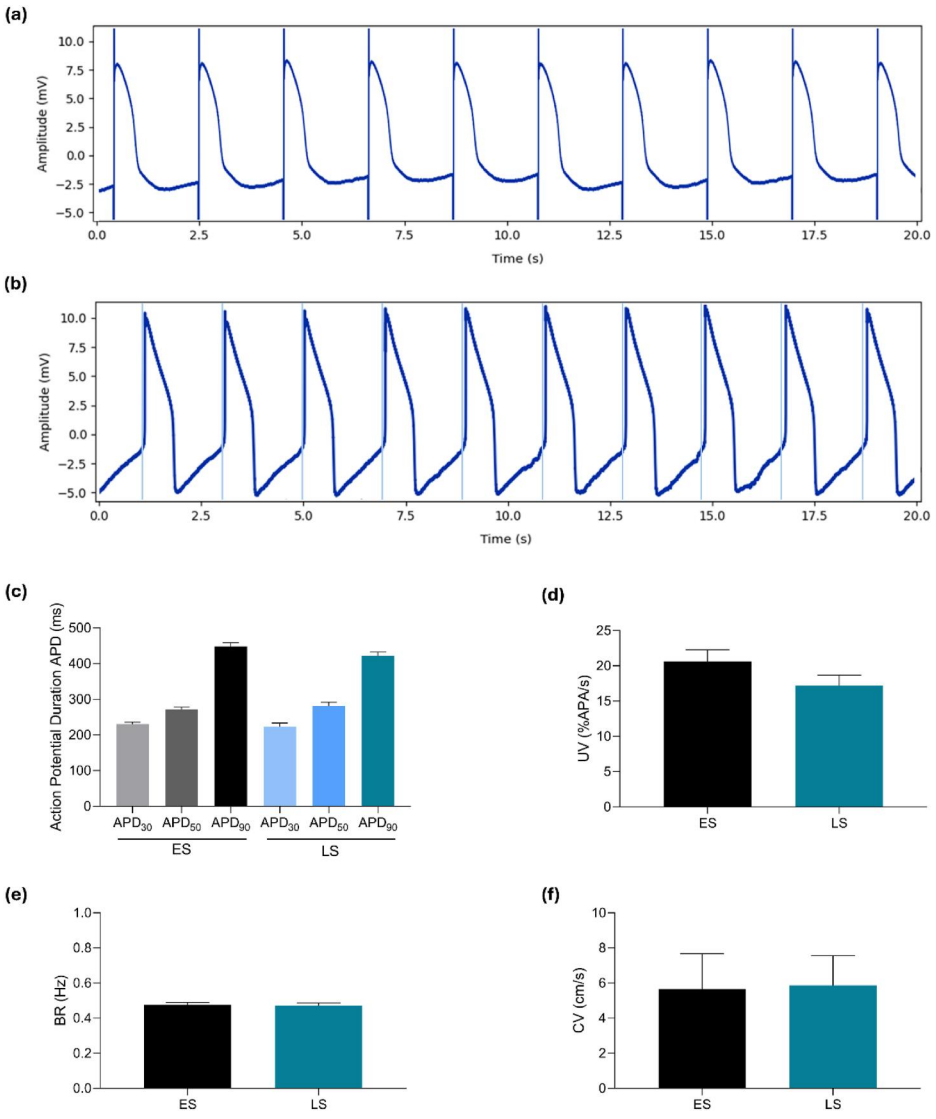

FIG. 3. Comparison between electrical and optical stimulation at 0.5 Hz in Ziapin2-loaded hiPSC-CMs. (a) Representative action potential (AP) traces evoked by electrical pacing at 0.5 Hz (bipolar stimulus, 1 ms pulse). (b) Representative light-induced APs in hiPSC-CMs incubated with 25 μM Ziapin2 and photostimulated at 0.5 Hz (100 ms pulse). Cyan shaded lines represent light stimulation. Quantification of (c) AP duration at different degrees of repolarization (APD_{30}, APD_{50}, and APD_{90}), (d) estimated upstroke velocity [UV, expressed as %AP amplitude (APA)/s], (e) beating rate (BR) and (f) conduction velocity (CV) in hiPSC-CMs paced either electrically (ES) or optically (LS). All recordings were performed at 37 °C. Data are presented as mean ± SEM ($30 \leq n \leq 71$ per condition, $N = 4$ independent differentiations).

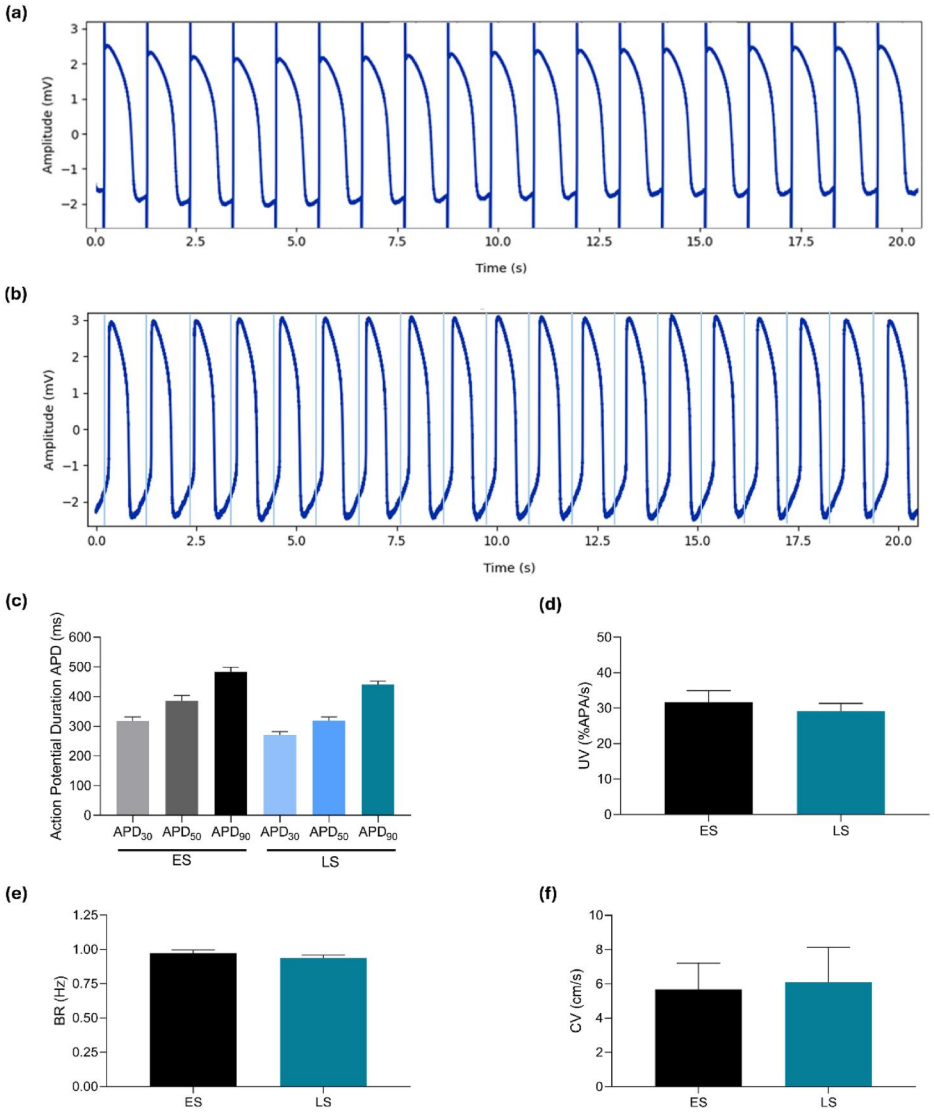

FIG. 4. Functional characterization of electrical and light-induced excitation at 1 Hz in hiPSC-CMs. (a) Representative action potential (AP) traces evoked by electrical pacing at 1 Hz (bipolar stimulus, 1 ms pulse). (b) Representative light-induced APs in hiPSC-CMs incubated with 25 μM Ziapin2 and photostimulated at 1 Hz (100 ms pulse). Cyan shaded lines represent light stimulation. Quantification of (c) AP duration (APD_{30}, APD_{50}, and APD_{90}), (d) estimated upstroke velocity [UV, expressed as %AP amplitude (APA)/s], (e) beating rate (BR) and (f) conduction velocity (CV) in hiPSC-CMs paced either electrically (ES) or optically (LS). All recordings were performed at 37 °C. Data are presented as mean ± SEM ($39 \leq n \leq 63$ per condition, $N = 4$ independent differentiations).

Notably, Ziapin2-mediated activation remained effective even at 1 Hz (Fig. 4), indicating that the photoisomerization kinetics of the molecule are sufficiently fast to follow physiological pacing rates without significant latency. This comparison confirms that the photophysical response of Ziapin2 enables temporally precise and repeatable control of CM depolarization, validating its use as a fully contactless alternative to electrical stimulation.

Importantly, the platform enabled stable intracellular recordings over multiple days *in vitro* (up to 1 week), with AP waveforms maintaining high signal-to-noise ratios and conserved morphological features (Fig. S3). At later time points, a moderate reduction in AP amplitude was sometimes observed, likely due to progressive detachment of contracting cells from the MEA substrate (data not shown). This effect may be mitigated by optimizing substrate coatings to enhance hiPSC-CM adhesion, for example, using extracellular matrix-based coatings such as Geltrex or laminin to improve long-term culture stability.[21] These results underline the prolonged optical responsiveness of Ziapin2 over time as well as the reliability and stability of the optoelectronic platform, which allows repeated laser poration at later time points in an effective manner. This dual-modality system delivers a robust, minimally invasive, and contactless means for extended high-fidelity electrophysiological recordings in human cardiac models, making it a valuable tool for applications such as drug screening and disease modeling.

To illustrate this capability, we performed pharmacological validation experiments using reference compounds with well-established electrophysiological effects. Specifically, we tested E4031, an I_{Kr} blocker known to prolong repolarization, and Nifedipine, an L-type Ca^{2+} channel blocker that shortens the AP. Both drugs were applied at increasing concentrations, revealing clear dose-dependent modulation of the recorded signals (Fig. 5). These results demonstrate the ability of the platform to capture expected pharmacological responses

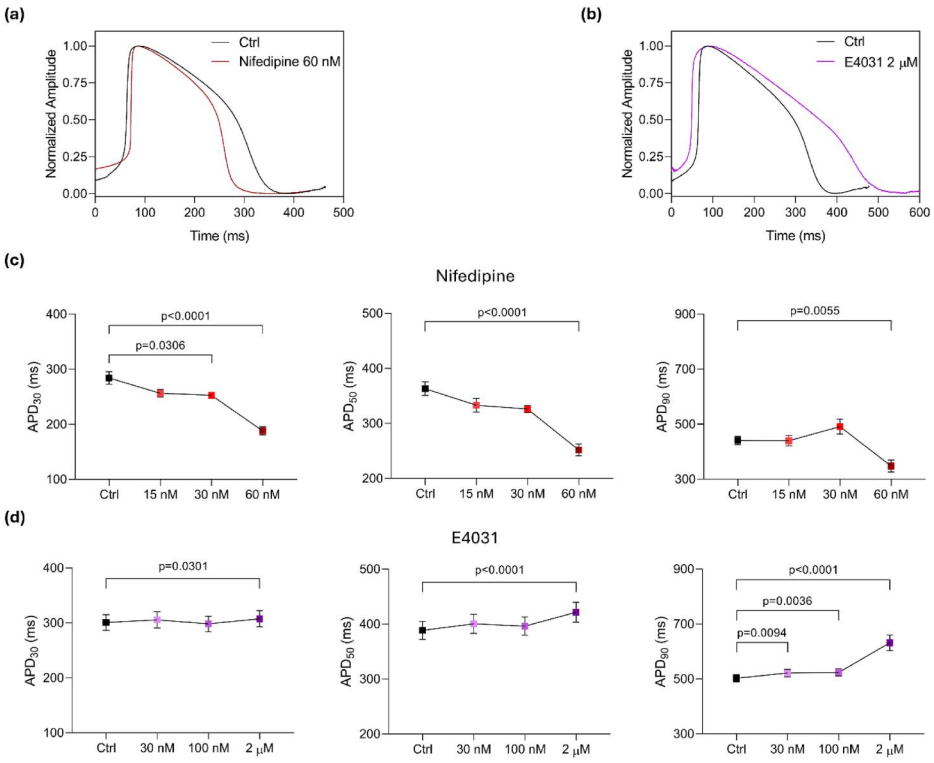

FIG. 5. Pharmacological modulation of hiPSC-CM AP recorded with the opto-electronic platform. (a) Representative AP comparison between control conditions (Ctrl, black) and treatment with Nifedipine (60 nM, red), showing shortening of the repolarization phase. (b) Representative AP comparison between Ctrl (black) and E4031 (2 μM, purple), illustrating prolongation of repolarization. (c) Quantification of AP duration at 30%, 50%, and 90% repolarization (APD_{30}, APD_{50}, and APD_{90}), following increasing concentrations of Nifedipine (15, 30, and 60 nM). (d) Quantification of APD_{30}, APD_{50}, and APD_{90} following increasing concentrations of E4031 (30, 100 nM, and 2 μM). Data are presented as mean ± SEM ($17 \leq n \leq 33$ per condition, obtained from a single differentiation).

across multiple experimental conditions, supporting its suitability for scalable electrophysiological screening.

C. Automated analysis of electrophysiological signals

Analyzing the wealth of electrophysiological data generated by our multimodal platform can be time-consuming, especially when dealing with complex experimental designs. To address this, we developed Action Potential Profiler (APP), a custom software suite for the automated analysis of electrophysiological signals from cardiac cultures grown on MEAs (Fig. 6). All quantitative analyses presented earlier were performed using APP and validated by comparison with manually analyzed data. The software is designed to handle intracellular APs, requiring minimal user intervention while ensuring high reproducibility. This streamlines data interpretation and is particularly suited for high-throughput experimental workflows. The software accepts input files in .hdf5 format, generated from MEA recordings acquired using the Multi-Channel Systems (MCS) platform. It supports both single-file and batch processing modes, allowing multiple datasets to be analyzed simultaneously. Before analysis, recordings can be filtered using various digital filters such as Bessel high- or low-pass, Notch, or Savitzky–Golay filters. These filtering options primarily serve to reduce high-frequency noise components, such as those around 50 Hz, thereby improving the signal-to-noise ratio. They can also mitigate slow baseline drifts or other low-frequency artifacts that may occasionally arise from electrode or recording instability. Each dataset can be analyzed as a whole or within user-defined time windows, enabling focused investigation of specific experimental phases, for example after laser poration or drug treatment. Users can also specify the biological model type, such as monolayers or organoids, to ensure that the software adapts to different signal morphologies and spatiotemporal dynamics. At the core of APP's functionality is its ability to extract a broad range of quantitative features from AP waveforms.

These include AP duration measured at 30%, 50%, and 90% repolarization levels (APD_{30}, APD_{50}, and APD_{90}), the beating rate (BR) and its variability across electrodes, an estimated upstroke velocity (UV), which serves as a proxy for depolarization speed, and conduction velocity (CV). APD values were defined as the time interval between the time points at which the upstroke and the repolarization phases cross the amplitude level at 30%, 50%, or 90% of the repolarization amplitude. For the calculation of the APD_{90}, in case the amplitude level fell below the upstroke curve, the same initial time point of the APD_{50} is used. CV was estimated from activation time differences between neighboring electrodes, calculated from the temporal delay of the AP upstroke across the electrode array and divided by the known inter-electrode distance.

These metrics are computed for individual APs and then averaged per electrode and per well. APP also generates detailed visual outputs, including mean AP waveforms averaged over consecutive beats, bar plots comparing single APs to these averages, time-resolved traces following laser poration, and electrode-specific APD comparisons along with statistical summaries. A key feature is the electrode selection panel, which allows users to view and analyze signals from specific channels. The software organizes all outputs into a structured data repository, with folders categorized by data type (such as APD, extracted curves, signals, single APs, and other values), saving results in both graphical (png) and tabular (.csv, .xls) formats. At the culture

FIG. 6. Main window of the analysis software Action Potential Profiler (APP). The red squares highlight the main results of the analysis of APs acquired with IntraCell and MEA systems. (a) Mean AP of the selected electrode, normalized; (b) main parameters of the mean AP, including APD_{30}, APD_{50}, and APD_{90}, estimated upstroke velocity, beating rate, and standard deviations; (c) specific AP selected in the analyzed electrode trace, normalized; (d) time course of APs from the selected electrode; and (e) comparison between the mean AP and the selected AP.

level, the overview window aggregates electrophysiological activity across the entire preparation, offering a preview of the nine highest quality signals alongside heatmaps of key metrics (i.e., BR, CV, UV, and APD at various repolarization levels), including their standard deviations (Fig. S4). These visualizations help identify spatial heterogeneities within the MEA and provide rapid insight into the overall electrophysiological status of the culture, including the presence of arrhythmogenic foci or conduction blocks. The comparison window facilitates pairwise or multi-condition analyses of previously processed datasets (Fig. S5). Users can compare AP waveforms and APD metrics across different electrodes, wells, or experimental conditions (for example, before and after treatment or at multiple time points). This feature is especially valuable in longitudinal studies or pharmacological assays where quantitative tracking of changes over time is critical. APP also allows users to add annotations and metadata to each analysis and to generate comprehensive PDF reports summarizing waveform features, parameter distributions, and heatmaps.

III. CONCLUSIONS AND FUTURE PERSPECTIVES

In this work, we successfully demonstrated the prototype of a versatile optoelectronic platform combining optical pacing with high-fidelity intracellular recordings enabled by laser poration. While this study specifically employed Ziapin2 to control bioelectricity in a hiPSC-CM monolayer, the system is highly tunable and adaptable to various experimental needs. Specifically, (i) the platform might be exploited with a broad spectrum of photostimulation techniques, including optogenetics, caged compounds, photoactivatable drugs, and photonic devices.[22] This versatility enables the adoption of diverse optical control strategies, making the platform suitable for a wide range of experimental approaches in biophysics and bioengineering; (ii) although for this proof-of-principle study, we used two-dimensional hiPSC-CM monolayers cultured on planar MEAs, the technology is inherently scalable and can be readily adapted to more complex three-dimensional cardiac models, such as organoids or cardioids.[23–28] This adaptability enables studies in systems that more closely mimic physiological conditions, broadening the range of biologically relevant investigations; (iii) while the current platform uses a cyan (470 nm) LEDs for photostimulation, the platform architecture enables straightforward replacement with modules emitting at alternative wavelengths. Looking ahead, integrating a broadband, fiber-coupled illumination system (e.g., Lumencor Spectra X) could provide rapid switching among multiple wavelength channels, further expanding the platform's utility for diverse applications. Such enhancements would expand excitation capabilities across the visible spectrum, increasing compatibility with a broader portfolio of photo-transducers and optogenetic constructs; (iv) even if the integrated software provides robust, automated functionalities for high-throughput and structured analysis of electrophysiological datasets, future development will focus on enabling customizable report generation to further enhance analytical flexibility and user experience. Taken together, our platform represents a powerful resource for scalable, high-throughput cardiac research, with broad applicability in drug screening, including pharmacological dose–response studies with ion channel blockers, disease modeling using patient-specific hiPSC-CMs, and chronic pacing studies where large datasets and reproducibility are paramount.

IV. MATERIALS AND METHODS

A. Culture and differentiation of human-induced pluripotent stem cell-derived cardiomyocytes

Bona fide healthy, human-induced pluripotent stem cells (hiPSCs) from the WTC-11 hiPSC line (hPSCReg UCSFi001-A) were obtained with appropriate Material Transfer Agreement from the Coriell Institute for Medical Research (No. GM25256). HiPSCs were cultured on plastic multiwell plates coated with recombinant human vitronectin (rhVTN, Thermo Fisher Scientific, A14700) in Essential 8 Flex medium (Thermo Fisher Scientific, A2858501). HiPSCs were plated on hESC qualified Matrigel (BD Biosciences, 354277) before cardiac differentiation and differentiated to hiPSC-CMs following a protocol based on the modulation of the Wnt signaling pathway[29] with minor modifications. hiPSC-CMs were purified through glucose starvation (final purity > 90% CMs) and cryopreserved on days 9–16. Cryopreserved hiPSC-CMs were thawed, expanded, and maintained in medium containing RPMI1640 medium (Euroclone, ECB2000) supplemented with B27 Supplement (Thermo Fisher, 17504044) and 1% KnockOut Serum Replacement (Thermo Fisher Scientific, 10828028). hiPSC-CMs were dissociated using TrypLE 1X (Thermo Fisher Scientific, 12604013) and plated on 40 μg/ml bovine fibronectin-coated (Merck, F1141) glass MicroElectrode Arrays (MEAs) at a density of $\sim 5 \times 10^4$ cells/well (6-well) or $\sim 1.5 \times 10^5$/well (single-well). Medium was refreshed every other day until the experimental day.

B. Ziapin2 synthesis and internalization process

Ziapin2 was synthesized following previously published procedures[13,30] and administered directly to hiPSC-CMs by adding it to the culture medium.[19] Specifically, hiPSC-CMs were incubated with 25 μM Ziapin2 at 37 °C and 5% CO_2 for 7 min. After incubation, excess compound was gently washed out, and the cultures were rinsed with fresh culture medium before proceeding with further analysis.

C. Microelectrode array (MEA) recordings

All recordings from MCS-MEAs were performed at 37 °C outside the incubator. The cell medium from each sample was changed 2 h before the measurements. MEA recordings were obtained with a MEA2100-Mini-System from the company Multi-Channel Systems MCS GmbH. Recordings with the MEA2100-Mini-System were acquired at 20 kHz acquisition frequency, high-pass hardware filtering of 0.1 Hz, and low-pass hardware filtering of 10 kHz.

D. Laser-based cellular optoporation

Laser pulse trains were applied on the surface of MCS-MEAs to porate hiPSC-CMs. For laser poration, the IntraCell system uses the protocol originally introduced by Dipalo and coworkers.[31] The average laser power during the optoporation protocol was 5 mW. The laser was coupled to an inverted optical setup able to accommodate the acquisition system MEA2100-Mini from Multi-Channel Systems MCS GmbH. A 20× air objective (NA = 0.42, working distance = 6 mm) was used during the experiments to observe the cells on the devices and to focus the NIR laser used for poration.

To produce programmable optical stimulation patterns with IntraCell, we use a combination of a I2C Digital-to-Analog Converter (DAC) (MCP4725) and a LED Driver (MP24833-A). The first device, MCP4725, receives digitally the stimulation pattern desired by the user in terms of amplitude, repetition rate, and duty cycle and converts this information into an analog voltage signal. The second device (MP24833-A) is voltage-controlled current source. It takes the analog voltage from the MCP4725 device and delivers a proportional current to the 470 nm LED light source.

E. Photostimulation of Ziapin2

Illumination of hiPSC-CM cultures during electrophysiological experiments was provided by a collimated light-emitting diode (LED, Thorlabs), integrated into the IntraCell system, as detailed in the manuscript. The light source was characterized by a maximum emission wavelength of 470 nm to match the molecule absorption spectrum. The illuminated spot on the sample has an area of 0.8 mm^2 and a maximum photoexcitation density of 14 mW/mm^2.

F. Custom-made analysis algorithm

The data were analyzed using the custom-made analysis algorithm APP. The algorithm allows for accurate characterization of the intracellular APs waveforms, the intracellular APs duration at different amplitude values with respect to the maximum amplitudes (30%, 50%, and 90%), and the beating rate. In figures, data were plotted as mean ± standard error of the mean (SEM). Data normality were assessed using the D'Agostino–Pearson normality test. Comparisons between the two groups were performed using either Student's *t*-test or the Mann–Whitney U test, as appropriate. Comparisons among more than two independent groups were conducted using one-way ANOVA followed by Dunnett's post hoc test or the Kruskal–Wallis test with Dunn's correction for multiple comparisons. Paired comparisons across multiple conditions were analyzed using the Friedman test followed by Dunn's multiple comparisons test. When statistically significant differences were observed, the exact p-values are reported in the corresponding figures. For each experiment, the number of technical replicates (n, electrodes from different MEAs) and biological replicates (N, independent differentiations) are reported in the corresponding figure legend.

SUPPLEMENTARY MATERIAL

See the supplementary material for the following: Fig. S1: Representative extracellular field potential recordings showing light-induced modulation of electrical activity in hiPSC-CMs treated with Ziapin2, compared to vehicle-treated controls. Fig. S2: Graphical user interface of the FB Alps software suite used for optical stimulation and MEA control, including modules for imaging, laser targeting, electrode selection, and experimental parameter configuration. Fig. S3: Long-term functional stability of optically evoked activity in Ziapin2-loaded hiPSC-CMs, including representative traces and quantitative analysis of electrophysiological parameters (APD, upstroke velocity, beating rate, and conduction velocity). Fig. S4: Overview window of the APP software, showing representative electrophysiological traces and spatial heatmaps of key functional parameters across the preparation. Fig. S5: Comparison module of the APP software, enabling cross-dataset analysis through waveform superposition and statistical comparison of action potential features across electrodes and wells.

ACKNOWLEDGMENTS

The authors would like to thank Alessia Metallo for Fig. 2. This research was supported by the Italian Ministry of Universities and Research through the PRIN 2022 project (ID 2022-NAZ-0595) to F.L., the PRIN 2020 project (ID 2020XBFEMS) awarded to C.B. and G.L., and the Fondo Italiano per la Scienza project (ID FIS00001244) to G.L. This research was partly supported by the European Innovation Council (EIC) through the SiMulTox project (GA: 101057769) within the framework of Horizon Europe to M.D. Additional support was provided by the Italian Ministry of University and Research within Mission 4, "Education and Research," Component 2, "From Research to Business," and Investment 1.2, "Funding projects presented by young researchers" of the National Recovery and Resilience Plan, Project No. 2022-NAZ-0485 (H45E22001210006) to LS.

AUTHOR DECLARATIONS

Conflict of Interest

G.L., C.B., and F.L. are inventors of "PHOTOCHROMIC COMPOUNDS" (Patent No. EP 3802491) (02/07/2020). M.D. is a co-inventor of "Method and device for recording intracellular action potentials in electrogenic cells" (Patent No. EP3724655B1) (12/12/2018).

Ethics Approval

This study was conducted in accordance with the Declaration of Helsinki, and ethical approval was granted by the Ethics Committee of Istituto Auxologico Italiano IRCCS. Appropriate informed consent was obtained from all the donors.

Author Contributions

Chiara Florindi: Conceptualization (equal); Data curation (equal); Formal analysis (equal); Investigation (equal); Methodology (equal); Validation (equal); Visualization (equal); Writing – original draft (equal). **Carolina Scandellari:** Software (equal); Writing – review & editing (equal). **Claudia Maniezzi:** Formal analysis (equal); Writing – review & editing (equal). **Giulia Bruno:** Formal analysis (equal); Writing – review & editing (equal). **Luca Sala:** Methodology (equal); Resources (equal); Writing – review & editing (equal). **Annarita Di Mise:** Methodology (equal); Writing – review & editing (equal). **Guglielmo Lanzani:** Funding acquisition (equal); Writing – review & editing (equal). **Chiara Bertarelli:** Funding acquisition (equal); Resources (equal); Writing – review & editing (equal). **Marcella Rocchetti:** Methodology (equal); Writing – review & editing (equal). **Antonio Zaza:** Methodology (equal); Supervision (equal); Writing – review & editing (equal). **Michele Dipalo:** Data curation (equal); Methodology (equal); Software (equal); Supervision (equal); Writing – review & editing (equal). **Francesco Lodola:** Conceptualization (equal); Data curation (equal); Funding acquisition (equal); Investigation (equal); Methodology (equal); Supervision (equal); Validation (equal); Visualization (equal); Writing – original draft (equal).

DATA AVAILABILITY

The data that support the findings of this study are available from the corresponding authors upon reasonable request.

REFERENCES

[1]D. M. Bers, "Cardiac excitation–contraction coupling," Nature **415**, 198 (2002).
[2]M. Prondzynski, P. Berkson, M. A. Trembley, Y. Tharani, K. Shani, R. H. Bortolin, M. E. Sweat, J. Mayourian, D. Yucel, A. M. Cordoves, B. Gabbin, C. Hou, N. J. Anyanwu, F. Nawar, J. Cotton, J. Milosh, D. Walker, Y. Zhang, F. Lu, X. Liu, K. K. Parker, V. J. Bezzerides, and W. T. Pu, "Efficient and reproducible generation of human iPSC-derived cardiomyocytes and cardiac organoids in stirred suspension systems," Nat. Commun. **15**(1), 5929 (2024).
[3]H. Yang, Y. Yang, F. N. Kiskin, M. Shen, and J. Z. Zhang, "Recent advances in regulating the proliferation or maturation of human-induced pluripotent stem cell-derived cardiomyocytes," Stem Cell Res. Ther. **14**, 228 (2023).
[4]J. Li, Y. Hua, S. Miyagawa, J. Zhang, L. Li, L. Liu, and Y. Sawa, "hiPSC-derived cardiac tissue for disease modeling and drug discovery," Int. J. Mol. Sci. **21**-(23), 8893 (2020).
[5]K. Kadan-Jamal, F. Wronowski, A. Jin, T. E. Naegele, V. R. Montes, X. Tao, A. Dominguez-Alfaro, C. Lee, and G. G. Malliaras, "Electrical stimulation of cells: Drivers, technology, and effects," Chem. Rev. **125**(15), 6874–6905 (2025).
[6]C. Florindi, G. Simoncini, G. Lanzani, and F. Lodola, "Shining light in a heartbeat: Controlling cardiac bioelectricity with membrane-targeted photoswitches," Appl. Phys. Lett. **126**(23), 230501 (2025).
[7]V. Vurro, I. Venturino, and G. Lanzani, "A perspective on the use of light as a driving element for bio-hybrid actuation," Appl. Phys. Lett. **120**(8), 080502 (2022).
[8]E. Entcheva and M. W. Kay, "Cardiac optogenetics: A decade of enlightenment," Nat. Rev. Cardiol. **18**(5), 349–367 (2021).
[9]G. Iachetta, N. Colistra, G. Melle, L. Deleye, F. Tantussi, F. De Angelis, and M. Dipalo, "Improving reliability and reducing costs of cardiotoxicity assessments using laser-induced cell poration on microelectrode arrays," Toxicol. Appl. Pharmacol. **418**, 115480 (2021).
[10]G. Iachetta, G. Melle, M. Dipalo, and F. De Angelis, "Long-term monitoring of cardiac action potentials for the assessment of chronic cardiotoxicity," J. Pharmacol. Toxicol. Methods **133**, 107633 (2025).
[11]J. Schaefer, T. Danker, K. Gebhardt, and U. Kraushaar, "Laser-induced action potential-like measurements of cardiomyocytes on microelectrode arrays for increased predictivity of safety pharmacology," J. Visualized Exp. **187**, 64355 (2022).
[12]L. Sala, D. Ward-van Oostwaard, L. G. J. Tertoolen, C. L. Mummery, and M. Bellin, "Electrophysiological analysis of human pluripotent stem cell-derived cardiomyocytes (hPSC-CMs) using multi-electrode arrays (MEAs)," J. Visualized Exp. **123**, 55587 (2017).
[13]M. L. DiFrancesco, F. Lodola, E. Colombo, L. Maragliano, M. Bramini, G. M. Paternò, P. Baldelli, M. D. Serra, L. Lunelli, M. Marchioretto, G. Grasselli, S. Cimò, L. Colella, D. Fazzi, F. Ortica, V. Vurro, C. G. Eleftheriou, D. Shmal, J. F. Maya-Vetencourt, C. Bertarelli, G. Lanzani, and F. Benfenati, "Neuronal firing modulation by a membrane-targeted photoswitch," Nat. Nanotechnol. **15**(4), 296–306 (2020).
[14]G. M. Paternò, E. Colombo, V. Vurro, F. Lodola, S. Cimò, V. Sesti, E. Molotokaite, M. Bramini, L. Ganzer, D. Fazzi, C. D'Andrea, F. Benfenati, C. Bertarelli, and G. Lanzani, "Membrane environment enables ultrafast isomerization of amphiphilic azobenzene," Adv. Sci. **7**(8), 1903241 (2020).
[15]F. Marangi, G. Simoncini, C. Florindi, F. Lodola, G. M. Paternò, and G. Lanzani, "A computational study of light-induced superimposed mechanical and dipolar effects," Eur. Phys. J. Plus **140**(9), 937 (2025).
[16]C. Florindi, A. Ostini, C. Bertarelli, J. P. Kucera, and F. Lodola, "Capacitance-driven modulation of cardiac impulse conduction by an intramembrane molecular photoswitch," Int. J. Mol. Sci. **26**(24), 11766 (2025).
[17]L. Cestariolo, C. Florindi, C. Bertarelli, A. Zaza, G. Lanzani, F. Lodola, and J. F. Rodriguez Matas, "Cardiac action potential generation mechanisms via an intramembrane photoswitch. A simulation study," Biophys. J. **124**, 4505 (2025).
[18]V. Vurro, B. Federici, C. Ronchi, C. Florindi, V. Sesti, S. Crasto, C. Maniezzi, C. Galli, M. R. Antognazza, C. Bertarelli, E. Di Pasquale, G. Lanzani, and F. Lodola, "Optical modulation of excitation-contraction coupling in human-induced pluripotent stem cell-derived cardiomyocytes," iScience **26**(3), 106121 (2023).

[19]C. Florindi, Y. Jang, K. Shani, P. Moretti, C. Bertarelli, G. Lanzani, K. K. Parker, F. Lodola, and V. Vurro, "A cardiac microphysiological system for studying Ca^{2+} propagation via non-genetic optical stimulation," J. Visualized Exp. **217**, e67823 (2025).
[20]C. Florindi, V. Vurro, P. Moretti, C. Bertarelli, A. Zaza, G. Lanzani, and F. Lodola, "Role of stretch-activated channels in light-generated action potentials mediated by an intramembrane molecular photoswitch," J. Transl. Med. **22**, 1068 (2024).
[21]A. Koc, S. Sahoglu Goktas, T. Akgul Caglar, and E. Cagavi, "Defining optimal enzyme and matrix combination for replating of human induced pluripotent stem cell-derived cardiomyocytes at different levels of maturity," Exp. Cell Res. **403**(2), 112599 (2021).
[22]C. M. Lopes, P. Barata, and R. Oliveira, "Chapter 5—Stimuli-responsive nanosystems for drug-targeted delivery," in *Drug Targeting and Stimuli Sensitive Drug Delivery Systems*, edited by A. M. Grumezescu (William Andrew Publishing, 2018), pp 155–209.
[23]A. Yaqinuddin, A. Jabri, A. Mhannayeh, B. Taftafa, M. Alsharif, T. Abbad, J. Khan, A. Elsalti, R. Chinnappan, E. A. Alshehri, A. Alzhrani, D. A. Obeid, I. Fujitsuka, M. Khan, M. U. Rehman, and T. A. Mir, "Cardiac organoids: A new tool for disease modeling and drug screening applications," Front. Cardiovasc. Med. **12**, 1537730 (2025).
[24]H.-Y. Zhao, J.-B. Jiang, S.-N. Wang, and C.-Y. Miao, "Technologies and applications of current human cardiac organoids," Acta Pharm. Sin. B **15**, 5734 (2025).
[25]E. Groen, C. L. Mummery, L. Yiangou, and R. P. Davis, "Three-dimensional cardiac models: A pre-clinical testing platform," Biochem. Soc. Trans. **52**(3), 1045–1059 (2024).
[26]Z. Huang, K. Jia, Y. Tan, Y. Yu, W. Xiao, X. Zhou, J. Yi, and C. Zhang, "Advances in cardiac organoid research: Implications for cardiovascular disease treatment," Cardiovasc. Diabetol. **24**(1), 25 (2025).
[27]R. Venkateshappa, Z. Yildirim, S. R. Zhao, M. A. Wu, F. Vacante, O. J. Abilez, and J. C. Wu, "Protocol to study electrophysiological properties of hPSC-derived 3D cardiac organoids using MEA and sharp electrode techniques," STAR Protoc. **5**(4), 103406 (2024).
[28]M. Miragoli, M. Burattini, A. Pisano, M. G. Pignataro, M. Dipalo, G. Orlandini, C. Scandellari, V. Medeghini, G. B. Luciani, G. Condorelli, and G. D' Amati, "Advancing cardiac 3D organoid-on-chip: Integrating iPSC-derived MELAS syndrome models to study electromechanical synchronicity and cardiac memory using contactless technology," Eur. Heart J. **45**(Supplement_1), ehae666.3675 (2024).
[29]X. Lian, J. Zhang, S. M. Azarin, K. Zhu, L. B. Hazeltine, X. Bao, C. Hsiao, T. J. Kamp, and S. P. Palecek, "Directed cardiomyocyte differentiation from human pluripotent stem cells by modulating Wnt/β-catenin signaling under fully defined conditions," Nat. Protoc. **8**(1), 162–175 (2013).
[30]V. Vurro, G. Bondelli, V. Sesti, F. Lodola, G. M. Paternò, G. Lanzani, and C. Bertarelli, "Molecular design of amphiphilic plasma membrane-targeted azobenzenes for nongenetic optical stimulation," Front. Mater. **7**, 10 (2021).
[31]M. Dipalo, G. Melle, L. Lovato, A. Jacassi, F. Santoro, V. Caprettini, A. Schirato, A. Alabastri, D. Garoli, G. Bruno, F. Tantussi, and F. De Angelis, "Plasmonic meta-electrodes allow intracellular recordings at network level on high-density CMOS-multi-electrode arrays," Nat. Nanotechnol. **13**(10), 965–971 (2018).